Assessment of Traumatic Brain Injury by Increased ^{64}Cu Uptake on $^{64}CuCl_2$ PET/CT

Fangyu Peng[1,2], Otto Muzik[3,4], Joshua Gatson[5], Steven G. Kernie[6], and Ramon Diaz-Arrastia[7]

[1]Department of Radiology, University of Texas Southwestern Medical Center, Dallas, Texas; [2]Advanced Imaging Research Center, University of Texas Southwestern Medical Center, Dallas, Texas; [3]Carman and Ann Adams Department of Pediatrics, School of Medicine, Wayne State University, Detroit, Michigan; [4]Department of Radiology, School of Medicine, Wayne State University, Detroit, Michigan; [5]Department of Surgery, University of Texas Southwestern Medical Center, Dallas, Texas; [6]Department of Pediatrics and Department of Pathology and Cell Biology, Columbia University College of Physicians and Surgeons, New York, New York; and [7]Center for Neurosciences and Regenerative Medicine, Uniformed Services University of the Health Sciences, Bethesda, Maryland

Copper is a nutritional trace element required for cell proliferation and wound repair. **Methods:** To explore increased copper uptake as a biomarker for noninvasive assessment of traumatic brain injury (TBI), experimental TBI in C57BL/6 mice was induced by controlled cortical impact, and ^{64}Cu uptake in the injured cortex was assessed with $^{64}CuCl_2$ PET/CT. **Results:** At 24 h after intravenous injection of the tracer, uptake was significantly higher in the injured cortex of TBI mice (1.15 ± 0.53 percentage injected dose per gram of tissue [%ID/g]) than in the uninjured cortex of mice without TBI (0.53 ± 0.07 %ID/g, $P = 0.027$) or the cortex of mice that received an intracortical injection of zymosan A (0.62 ± 0.22 %ID/g, $P = 0.025$). Furthermore, uptake in the traumatized cortex of untreated TBI mice (1.15 ± 0.53 %ID/g) did not significantly differ from that in minocycline-treated TBI mice (0.93 ± 0.30 %ID/g, $P = 0.33$). **Conclusion:** Overall, the data suggest that increased ^{64}Cu uptake in traumatized brain tissues holds potential as a new biomarker for noninvasive assessment of TBI with $^{64}CuCl_2$ PET/CT.

Key Words: traumatic brain injury; copper metabolism; neuroimaging; positron emission tomography; ^{64}Cu-chloride

J Nucl Med 2015; 56:1252–1257
DOI: 10.2967/jnumed.115.154575

Traumatic brain injury (TBI) is a significant cause of neurologic disability among the U.S. population, affecting those who are in car accidents, involved in contact sports, or exposed to a blast on the battlefield (*1*). Neuroimaging plays an important role in the diagnosis and clinical management of TBI patients. Among the neuroimaging modalities, CT is useful for evaluating head injury features such as hemorrhages and edema (*2,3*); MR imaging is useful when neurologic symptoms are unexplained by the CT findings, because of higher sensitivity for microhemorrhages and subtle nonhemorrhagic lesions (*4,5*); and PET is highly sensitive and quantitative in the assessment of brain perfusion (*6*) and changes in cerebral glucose metabolism (*7,8*). Because the sensitivity and specificity of ^{18}F-FDG PET in TBI may be limited by abundant physiologic ^{18}F-FDG uptake in nontraumatized brain tissues, it is important to search for new biomarkers for PET assessment of TBI.

Copper is an essential nutrient for the function of many enzymes present in physiologic and pathophysiologic processes of mammals (*9,10*). The brain is the organ containing the second largest amount of copper in the human body (*11*), and copper plays an important role in normal brain physiology (*12*). Copper is required for wound repair and regeneration, and increased copper has been detected in wound tissue (*13,14*). The molecular mechanisms by which copper plays a role in wound repair are not fully understood but may be related to induction of vascular endothelial growth factor expression for angiogenesis (*15*) and to copper-containing molecules serving an essential function in cell proliferation in the wound-healing process. In response to TBI, there may be increased copper uptake by activated microglia secondary to posttraumatic neuroinflammation (*16*), copper/zinc superoxide dismutase (*17*), and potentially other copper transporters and chaperones defending oxidative damage (*18*).

We hypothesized that increased copper uptake in traumatized brain tissues may be tracked in vivo using radioactive copper and that increased uptake of ^{64}Cu may be applied as a biomarker to assess TBI using $^{64}CuCl_2$ PET/CT. This study tested our hypothesis by comparing cerebral uptake in 3 groups of mice: a group in which TBI was induced by controlled cortical impact (CCI), a normal control group without TBI, and a modified sham control group. In the modified sham procedure the skin was incised, and instead of the craniotomy performed in the regular sham control procedure, a small hole was drilled into the cranium to minimize cortical injury (*19*). To increase the strength of this control, after the hole had been drilled the mice received an intracortical injection of zymosan A. Although this modified sham control procedure may cause mild damage to brain tissue, we expected it to be less than that caused by the regular sham control procedure.

In an initial effort to differentiate uptake caused by the requirement for copper for wound healing from uptake caused by neuroinflammation, we assessed cerebral ^{64}Cu uptake in TBI mice treated and not treated with minocycline, a tetracycline derivative with antiinflammatory effects in TBI (*20*). The results of this comparison are expected to be useful not only to investigate the molecular mechanism by which TBI increases copper uptake but also to determine whether $^{64}CuCl_2$ is a useful tracer for detecting neuroinflammation in TBI

Received Feb. 12, 2015; revision accepted Jun. 17, 2015.
For correspondence or reprints contact: Fangyu Peng, Department of Radiology, University of Texas Southwestern Medical Center, 5323 Harry Hines Blvd., Dallas, TX 75390-9140.
E-mail: fangyu.peng@utsouthwestern.edu
Published online Jun. 25, 2015.

with PET/CT and monitoring the therapeutic effects of minocycline and other antineuroinflammation medications.

MATERIALS AND METHODS

Animals and Radiopharmaceuticals

Adult male C57BL/6 mice (12–13 wk old) were purchased from the animal resource center at the University of Texas Southwestern Medical Center. The mice were randomly assigned to 4 groups: a group in which TBI was induced by CCI ($n = 7$) and 3 control groups: one without TBI (normal controls, $n = 5$), a modified sham control group ($n = 7$), and a minocycline treatment control group ($n = 7$). ^{64}Cu produced via ^{64}Ni(p,n)^{64}Cu on a biomedical cyclotron was purchased from Washington University in the form of $^{64}CuCl_2$ in a 0.1 M HCl solution. The specific activity of ^{64}Cu was 255.3 ± 92.5 GBq (6.9 ± 2.5 Ci)/μmol. All small-animal experiments were conducted according to a protocol approved by the UT Southwestern Institutional Animal Care and Use Committee.

Procedures

TBI was induced using a modification of a previously described method (*21–23*). In brief, the mice were subjected to CCI using a Benchmark Stereotactic Impactor (Leica Microsystems) under 5% isoflurane anesthesia while in an adapted nosecone device. To maintain body temperature, each animal was placed on a heating pad and monitored using a rectal thermometer. The skin was incised to expose the skull, and a 5-mm-diameter craniotomy was performed to expose the right parietotemporal cortex. A 3-mm flat impactor tip was aligned, and an impact was delivered using the pneumatic cylinder at a velocity of 4.4 m/s to a depth of 1.3 mm with a dwell time of 100 ms. Afterward, the cranium was replaced and tightened with Loctite (Henkel Corp.). The incision was closed with surgical clips. The animals were treated with buprenorphine (0.05 mg/kg) before and 12 h after injury to reduce pain and then were monitored for pain every 6 h until 24 h and once daily thereafter. To maintain body temperature, a heating pad was placed under the cage for 24 h after surgery.

The modified sham controls underwent the same procedure as the TBI group with the exception of the CCI step. Instead, after incision of the scalp, a 2-mm hole was drilled into the cranium, and a 2-μL intracortical injection of zymosan A solution (25 mg/mL in normal saline) was administered using a modification of a previously described method (*24*).

The minocycline treatment controls underwent the same procedure as the TBI group with the addition of a 60 mg/kg intraperitoneally injected dose of minocycline in 0.1 mL of normal saline 30 min after the injury and then every 12 h for 4 d (*20*).

Small-Animal PET/CT

The CCI-induced TBI mice underwent $^{64}CuCl_2$ PET/CT 5 d after induction of the injury, along with the normal controls ($n = 5$), modified sham controls, and minocycline treatment controls. Imaging was performed with an Inveon system (Siemens) using a method described previously (*25,26*). Briefly, anesthesia was induced by inhalation of 3% isoflurane in 100% oxygen (3 L/min) at room temperature. The mice were placed in spread-supine position on the imaging bed, and anesthesia was maintained during the PET/CT procedure by inhalation of 2% isoflurane in 100% oxygen (3 L/min), using an isoflurane vaporizer (Summit Anesthesia Solutions). After the initial CT scan, the mice were injected via the tail vein with $^{64}CuCl_2$ at a dose of 74 kBq (2 μCi)/g of body weight as used previously (*25,26*), diluted into a total volume of 100 μL with normal saline (0.9% sodium chloride). A 30-min (5-min frames) dynamic whole-body data acquisition with the head in the center of the field of view began immediately afterward, followed by static imaging for 15 min at 2 and 24 h after injection. PET/CT images were reconstructed using 3-dimensional ordered-subsets expectation maximization and analyzed using Inveon Research Workplace software (Siemens), which allows fusion of CT and PET image volumes.

Quantitative Analysis of Brain ^{64}Cu Activity

Inveon Research Workplace software was used for quantitative analysis of the PET images. Because of the suboptimal anatomic resolution of CT images, regions of interest (ROIs) were manually drawn on the PET/CT images in reference to an MR imaging–based atlas of mouse brain anatomy (*27*). Seven ROIs were defined: injured cortex in TBI mice or the corresponding area in mice without TBI (ROI 1), contralateral cortex on the noninjured side of the brain (ROI 2), ipsilateral hippocampus inferior to the injury site (ROI 3), hippocampus on the contralateral site (ROI 4), ipsilateral thalamus (ROI 5), contralateral thalamus (ROI 6), and cerebellum (ROI 7), as shown in Figure 1. The percentage injected dose per gram of tissue (%ID/g) for these 7 ROIs was obtained by dividing the regional tracer concentration (kBq/cm^3) by the injected activity (kBq) and multiplying the result by 100% using Inveon Research Workplace software.

PET/MR Fusion Display of Brain ^{64}Cu Activity

To allow cerebral uptake to be viewed without interference from the intense activity at the craniotomy site (Figs. 1 and 2), an MR imaging–based atlas of normal C57BL/6 mouse brain (*27*) was coregistered to the CT images using a 7-parameter affine transformation (x,y,z translation, $\alpha\beta\gamma$ rotation, scaling). After coregistration, only activity overlying the MR atlas was retained, thus removing the intense activity in the scalp. This approach allowed detailed assessment of the uptake pattern in brain tissue relative to the anatomic landmarks provided by the atlas. All images were processed using AMIDE software (*28*).

Histologic Analysis

After undergoing imaging, the mice were placed in a room approved for housing animals injected with radiopharmaceuticals to allow complete decay of radionuclide activity (10 half-lives of ^{64}Cu = 127 h). Five

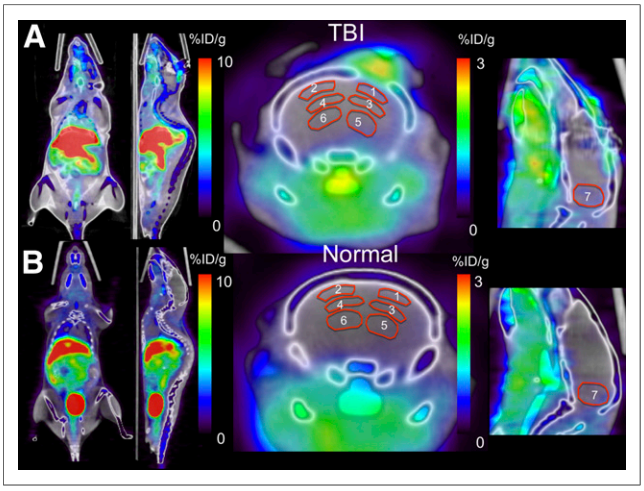

FIGURE 1. $^{64}CuCl_2$ PET/CT images showing biodistribution of ^{64}Cu. (A) TBI mouse shows intense physiologic activity in liver, as well as in kidney and intestine regions on left-sided whole-body images. Physiologic activity is also seen in soft tissue inferior to brain. Focally increased uptake was seen in craniotomy wound 2 h after injection. Activity pattern in brain tissue is poorly demonstrated because intensity scale is optimized to show whole-body biodistribution. (B) Mouse without TBI shows physiologic activity in liver, kidneys, and intestines and abundant activity in urinary bladder. ROIs for PET quantitative analysis are shown on right-sided coronal and sagittal views of brain.

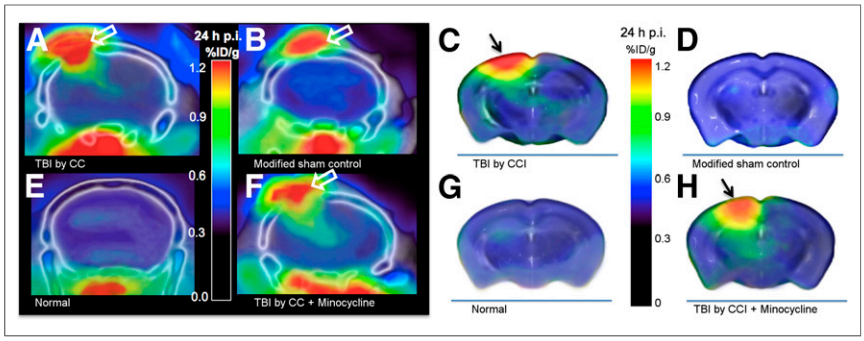

FIGURE 2. $^{64}CuCl_2$ PET/CT images showing increased activity in traumatized brain tissues. Focally increased activity is seen in untreated TBI mouse (A) and minocycline treatment control (F) but not in modified sham control (B) or normal control (E). Intense focal activity is seen in skin wound (A, B, and F), and physiologic uptake is seen in soft tissue inferior to skull base (A, B, E, and F). For better visualization of activity in brain tissues without spillover from skin wound, cerebral activity is schematically displayed using PET images overlaid on MR atlas of mouse brain. Locally increased uptake in injured brain tissues is seen in untreated TBI mouse (C) and minocycline treatment control (H). In contrast, uptake is not significantly increased in normal control (G) or modified sham control (D). Black arrows point to CCI injury, and white arrows to skin wound/craniotomy. p.i. = after injection.

days later, they were sacrificed using transcardiac perfusion with 4% formaldehyde in phosphate-buffered saline (PBS), followed by immersion fixation. The brains were removed, serially sectioned for the entire rostrocaudal axis, and paraffin-embedded, after fixation with paraformaldehyde. The brain tissues were sectioned (5-μm sections) and then were stained with hematoxylin and eosin for microscopic examination of traumatic damage to brain tissues. Expression of rabbit polyclonal antiionized calcium binding adapter molecule 1 (IBa1), a biomarker specific for microglia and macrophages, in brain tissues was assessed by immunohistochemical analysis using IBa1 antibody (WAKO Chemicals USA) in a modification of a previously described method (*29*). Briefly, the deparaffinized sections were microwaved in sodium citrate buffer (5 min × 2) to retrieve the antigen and incubated with 3% H_2O_2 in PBS for 5 min to inhibit endogenous peroxidase activity, washed in PBS, and blocked in PBS containing 1.5% normal blocking serum (ABC Kit PK-4001; Vector Laboratories) for 30 min. After incubation of the section slides with anti-IBa1 antibody (1:100 in PBS) for 2 h at room temperature, and with a biotinylated goat antirabbit IgG antibody (1:200 in PBS) for 1 h at room temperature, the immunoreactivity of IBa1 was revealed using ABC reagent (Vector Laboratories), diaminobenzidine tetrahydrochloride substrate, and hematoxylin counterstaining and was visually examined and semiquantitatively recorded as negative, mild, moderate, or intense, as described previously (*30*). Photomicrographs of the IBa1 immunoreactivity were taken using a microscope (Olympus) equipped with a digital camera (SPOT Imaging Solution).

Statistical Analysis

To determine whether uptake differs between the TBI mice and the 3 control groups, we applied a 3 × 7 mixed-design ANOVA, with the between-subjects factor representing the 4 groups and the within-subjects factor representing the 7 ROIs. After a significant overall test, pairwise 2-sample *t* tests were conducted to determine significant differences between groups. To correct for multiple comparisons, the least significant difference test was performed for the post hoc tests.

RESULTS

Whole-Body Biodistribution

Whole-body images showed intense activity in the liver and less activity in the brain and muscles (Fig. 1 and Supplemental Table 1; supplemental materials are available at http://jnm.snmjournals.org), similar to previous findings (*25*). At 30 min after injection, focally increased activity in the craniotomy wound was seen for the TBI mice (3.20 ± 0.56 %ID/g) and the modified sham controls (3.00 ± 1.43 %ID/g), compared with the normal controls (0.41 ± 0.21 %ID/g) (Fig. 1 and Supplemental Table 1).

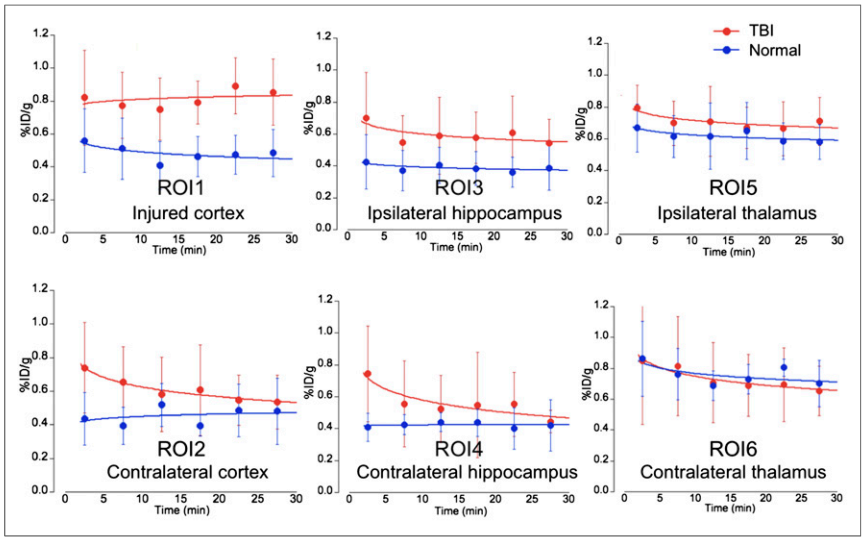

FIGURE 3. Time–activity curves of brain uptake on dynamic $^{64}CuCl_2$ PET/CT. Uptake was higher in TBI cortex than in contralateral cortex or corresponding region in normal controls. Uptake was minimally higher in ipsilateral TBI hippocampus than in contralateral hippocampus or corresponding region in normal controls. In contrast to the continuous increase in uptake in TBI cortex and ipsilateral hippocampus, activity gradually declined in other brain regions of TBI mice (ROIs 2, 4, 5, and 6), which reached same level as in normal controls by end of the 30-min dynamic PET analysis.

^{64}Cu Uptake in Untreated Traumatized Brain Tissues

In addition to the intense focus in the craniotomy wound (Figs. 2A and 2B), increased activity in traumatized brain tissue inferior to the craniotomy wound was seen for TBI mice (Fig. 2A) but not for normal controls (Fig. 2E) or modified sham controls (Fig. 2B). Focally increased activity was seen in the injured cortex (Fig. 2C) but not in the uninjured cortex contralateral to the CCI site in TBI mice (Fig. 2C), the cortex in normal controls (Fig. 2G), or the cortex in modified sham controls (Fig. 2D). Activity was also increased in the ipsilateral hippocampus inferior to the CCI injury (Fig. 2C) but not the contralateral hippocampus (Fig. 2C) or the hippocampus of the normal controls (Fig. 2G) or modified sham controls (Fig. 2D).

Dynamic imaging for 30 min after tracer injection showed that, compared with

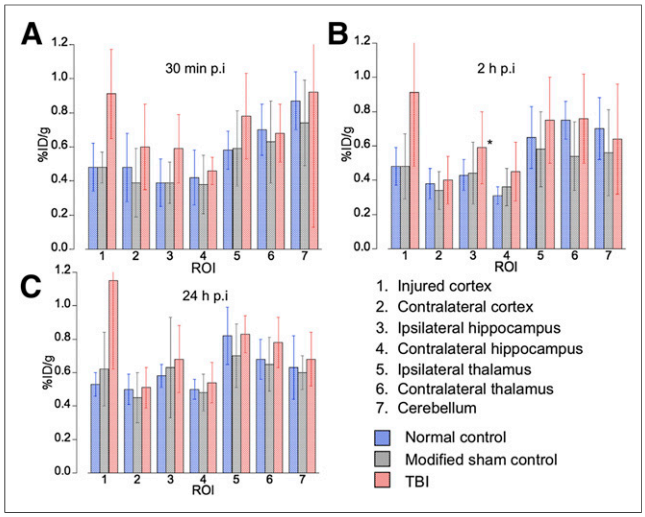

FIGURE 4. Quantification of increased ^{64}Cu uptake in traumatized brain tissues on $^{64}CuCl_2$ PET/CT. Uptake increased significantly in TBI mice, compared with normal controls or corresponding region in modified sham controls, at 30 min, 2 h, and 24 h after injection, respectively. p.i. = after injection.

physiologic uptake in the uninjured contralateral cortex, there was a gradual increase in uptake in the traumatized cortex as well as uptake in the corresponding uninjured regions of the normal controls and modified sham controls (Fig. 3). At 30 min after injection, focal activity was significantly higher in the injured cortex (0.91 ± 0.26 %ID/g) than in the contralateral uninjured cortex (0.60 ± 0.25 %ID/g, $P = 0.005$) or in the corresponding region of normal controls (0.48 ± 0.14 %ID/g, $P = 0.003$) or modified sham controls (0.48 ± 0.09 %ID/g, $P = 0.001$), as shown in Figure 4 and Supplemental Table 1. The static PET/CT imaging showed a continuous increase in uptake in the traumatized cortex (0.91 ± 0.43 and 1.15 ± 0.53 %ID/g at 2 and 24 h after injection, respectively), compared with the normal controls (0.48 ± 0.11 and 0.53 ± 0.07 %ID/g at 2 and 24 h after injection, respectively [$P = 0.047$ and 0.027]) or the modified sham controls (0.48 ± 0.19 and 0.62 ± 0.22 %ID/g at 2 and 24 h after injection, respectively [$P = 0.031$ and 0.025]), as seen in Figures 4B and 4C. Additionally, uptake was higher in the ipsilateral hippocampus inferior to the injured cortex than in the contralateral uninjured hippocampus or the normal or modified sham controls (Fig. 4; Supplemental Table 1).

^{64}Cu Uptake in Minocycline-Treated Traumatized Brain Tissues

Uptake in the traumatized cortex did not significantly differ between the minocycline treatment controls (Figs. 2F and 2H) and the TBI mice at 30 min or 2 h after injection of the tracer (Figs. 2A, 2C, and 5; Supplemental Table 1). At 24 h after injection, uptake in the traumatized cortex was slightly lower in the minocycline treatment controls (0.93 ± 0.30 %ID/g) than in the untreated TBI mice (1.15 ± 0.53 %ID/g), although this difference did not reach statistical significance ($P = 0.33$). Uptake in the other regions of the brain did not significantly differ between the untreated TBI mice and the minocycline treatment controls (Fig. 5; Supplemental Table 1). Furthermore, uptake in the craniotomy wound did not significantly differ between the TBI mice and the minocycline treatment controls at 30 min or 2 h after injection. At 24 h after injection, uptake in the craniotomy wound was slightly lower in the minocycline treatment controls (2.35 ± 0.73 %ID/g) than in the untreated TBI mice (2.86 ± 1.16 %ID/g), although, again, this small difference did not reach statistical significance ($P = 0.37$).

Immunohistochemical Analysis of IBaI for Microglial Activation

After hematoxylin and eosin staining of tissue sections, encephalomalacia was grossly visible at the injury site of TBI mice (Figs. 6A and 6F) but not in the uninjured brain of normal controls (Fig. 6E). Slight encephalomalacia derived from intracortical injection of zymosan A was seen in the tissue sections of modified sham controls (Fig. 6B). IBa1 immunoreactivity was detected in the injured cortex of TBI mice (Fig. 6C), indicating microglial activation. In contrast, the modified sham controls showed minimal immunoreactivity (Fig. 6D) and the normal controls showed none (Fig. 6G). Immunoreactivity was lower in the minocycline treatment controls (Fig. 6H) than in the untreated TBI mice (Fig. 6C).

DISCUSSION

Copper is a nutrient required for the function of many enzymes in humans. Radioactive copper was used for the preclinical study of copper metabolism in rodents using a small-animal PET/CT scanner (*25,26*). The whole-body biodistribution of ^{64}Cu in mice with or without TBI in the current study was similar to that of previous studies (*25,26*), with intense activity in the liver. As expected from an increased requirement for copper for wound healing, intense focal activity was seen at the craniotomy wound (Fig. 1). Focally increased uptake was seen in the traumatized cortex of TBI mice, compared with the contralateral cortex of these mice or the corresponding region in mice without TBI. Uptake did not significantly increase in modified sham controls, as was supported by minimal tissue injury and few IBa1-positive cells in the cortex surrounding the zymosan A injection site. The absence of neuroinflammation in the cortex of modified sham control mice, which received intracortical injection of zymosan A, was similar to previous findings in rats (*24*)

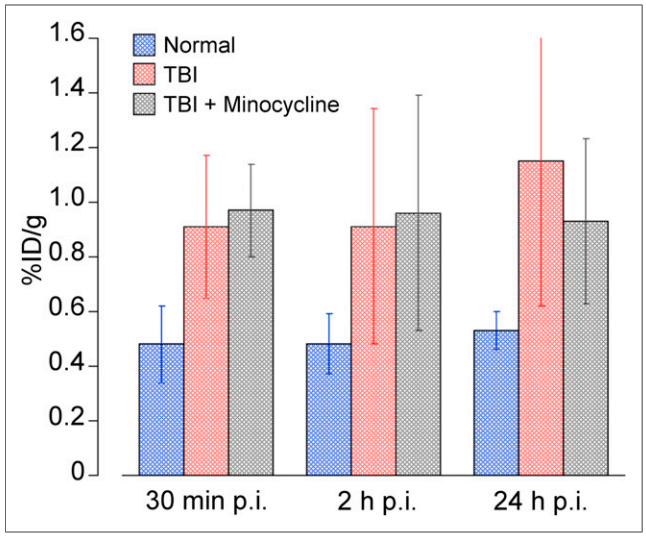

FIGURE 5. Effect of minocycline on ^{64}Cu uptake in injured cortex. Significantly increased uptake was detected in TBI mice with or without minocycline treatment, compared with normal controls. Uptake was not significantly decreased in minocycline treatment controls, compared with untreated TBI, at 30 min, 2 h, or 24 h after injection of $^{64}CuCl_2$. p.i. = after injection.

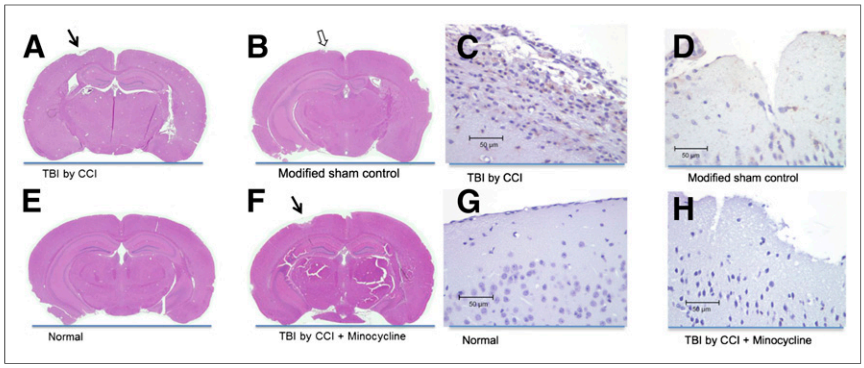

FIGURE 6. Hematoxylin and eosin staining and IBa1 immunoreactivity of injured cortex. Encephalomalacia is grossly visible in stained sections from TBI mice, whether treated (A) or not (F) with minocycline, but not in sections from mice without TBI (E). Staining shows minimal cortical damage in modified sham controls (B). IBa1-positive cells in injured cortex are more numerous in TBI mice (C) than in modified sham controls (D). There are no IBa1-positive cells in normal controls (G) and few, if any, in minocycline treatment controls (H), indicating the antineuroinflammatory activity of minocycline.

and different from findings when zymosan A was injected deeply into the corpus callosum (*31*). To the best of our knowledge, our study is the first to demonstrate increased radioactive copper uptake in CCI-induced experimental TBI, using a small-animal PET/CT scanner.

The molecular mechanisms of increased ^{64}Cu uptake in traumatized brain tissue remain to be elucidated. Compared with untreated TBI mice, the minocycline treatment controls showed decreased IBa1 immunoreactivity (Fig. 6D) but only a small decrease in ^{64}Cu uptake (0.93 ± 0.30 vs. 1.15 ± 0.53 %ID/g, $P = 0.33$) as shown in Figure 5. Our results suggest that increased uptake of ^{64}Cu in the traumatized brain tissues is likely caused by a combination of increased copper uptake by activated microglial cells (*16*), copper/zinc superoxide dismutase (*17*), and other copper transporters or chaperones (*12*). In view of the potential difference in neuroinflammation between the time of PET/CT and the time of postmortem brain tissue harvesting, 5 d after PET/CT, it would be ideal to correlate uptake and neuroinflammation with PET/CT using $^{64}CuCl_2$ and other tracers specific for biomarkers of neuroinflammation simultaneously (*31,32*).

Additional studies are also necessary to address a few issues. The first issue is that quantification of increased ^{64}Cu uptake in traumatized brain tissues in TBI mice may be confounded by disruption of the blood–brain barrier in these tissues. However, several lines of evidence suggest that the observed increase in uptake is likely caused by an increased demand for copper. Analysis of dynamic PET data demonstrates a time-dependent increase in uptake in traumatized cortex as compared with contralateral nontraumatized tissues, suggesting that the uptake is caused by a gradually increasing accumulation of copper, not simply by ^{64}Cu leakage due to blood–brain barrier disruption. The second issue is that it remains to be determined whether increased cerebral activity in the brains of the TBI mice quantified by PET reflects an increase in the absolute number of copper ions in brain tissue. Further validation may be possible by correlating activity measured by PET with the quantity of copper ions as determined by methods such as laser ablation inductively coupled plasma mass spectrometry (*33,34*). The third issue is that anatomic localization of activity measured in regions of the mouse brain by PET/CT may be subject to error given the small size of the brain and the spatial resolution of the small-animal PET/CT scanner.

Multiple positron-emitting copper isotopes are available for imaging copper metabolism with PET. These include ^{60}Cu ($t_{1/2}$ 23.7 min, 93% β^+, 7% electron capture), ^{61}Cu ($t_{1/2}$, 3.32 h, 60% β^+, 40% electron capture), ^{62}Cu ($t_{1/2}$, 9.74 m; 98% β^+, 2% electron capture), and ^{64}Cu ($t_{1/2}$, 12.7 h, 17.4% β^+, 43% electron capture, 39% β^-). ^{64}Cu has a physical decay half-life of 12.7 h, which allows shipping of ^{64}Cu radiopharmaceuticals from the production site to a remote imaging facility. Safe use of $^{64}CuCl_2$ as a radioactive tracer for noninvasive assessment of TBI in humans with PET/CT is supported by previous use of $^{64}CuCl_2$ to assess copper metabolism in healthy humans and Wilson disease patients (*35–37*); human radiation dosimetry estimates for $^{64}CuCl_2$ comparable to those for ^{18}F-FDG (*25*); minimal, if any, concern about the cytotoxicity of copper ions in view of the tiny amount of copper ions in a tracer dose of $^{64}CuCl_2$ compared with the amount of copper in a normal diet (*38*); and physiologic passage of ^{64}Cu through blood–brain barriers (*39*) mediated by human copper transporter 1 or other copper transport molecules in neurons (*12*). Considering the potential difference in copper response to injury between rodents and humans, the data from this preclinical study support clinical studies of $^{64}CuCl_2$ PET/CT for noninvasive assessment of TBI.

CONCLUSION

$^{64}CuCl_2$ PET/CT detected focally increased uptake in the traumatized cortex of CCI-induced TBI mice. The molecular mechanisms for the increased ^{64}Cu uptake in the traumatized brain tissues remain to be elucidated but are likely related to a nutritional requirement for copper ions for repair of CCI-induced TBI. The increased uptake of radioactive copper holds potential as a new biomarker for assessment of TBI with PET/CT.

DISCLOSURE

The costs of publication of this article were defrayed in part by the payment of page charges. Therefore, and solely to indicate this fact, this article is hereby marked "advertisement" in accordance with 18 USC section 1734. This research project was supported by the National Institutes of Health (7R21EB005331-03 and 1R21NS074394-01A). The production of ^{64}Cu at Washington University School of Medicine is supported by NCI grant R24 CA86307. No other potential conflict of interest relevant to this article was reported.

ACKNOWLEDGMENTS

We thank Saleh Ramezani for assistance with PET/CT and Rachel Sparks and Chengxi Li for assistance with histologic and immunohistochemical analysis of mouse brain tissues.

REFERENCES

1. Duckworth JL, Grimes J, Ling GS. Pathophysiology of battlefield associated traumatic brain injury. *Pathophysiology.* 2013;20:23–30.
2. Zee CS, Go JL. CT of head trauma. *Neuroimaging Clin N Am.* 1998;8:525–539.
3. Haydel MJ, Preston CA, Mills TJ, et al. Indications for computed tomography in patients with minor head injury. *N Engl J Med.* 2000;343:100–105.

4. Liu AY, Maldjian JA, Bagley LJ, et al. Traumatic brain injury: diffusion-weighted MR imaging findings. *Am J Neuroradiol.* 1999;20:1636–1641.
5. Yuh EL, Mukherjee P, Lingsma HF, et al. Magnetic resonance imaging improves 3-month outcome prediction in mild traumatic brain injury. *Ann Neurol.* 2013;73:224–235.
6. Coles JP, Fryer TD, Smielewski P, et al. Defining ischemic burden after traumatic brain injury using ^{15}O PET imaging of cerebral physiology. *J Cereb Blood Flow Metab.* 2004;24:191–201.
7. Hattori N, Huang SC, Wu HM, et al. Acute changes in regional cerebral ^{18}F-FDG kinetics in patients with traumatic brain injury. *J Nucl Med.* 2004;45:775–783.
8. García-Panach J, Nuria LN, Lull JJ, et al. A voxel-based analysis of FDG-PET in traumatic brain injury: regional metabolism and relationship between the thalamus and cortical areas. *J Neurotrauma.* 2011;28:1707–1717.
9. Linder MC. *Biochemistry of Copper.* New York, NY: Plenum Press; 1991.
10. Turnlund JR. Human whole body copper metabolism. *Am J Clin Nutr.* 1998;67 (suppl):960S–964S.
11. Lech T, Sadlik JK. Copper concentration in body tissues and fluids in normal subjects of southern Poland. *Biol Trace Elem Res.* 2007;118:10–15.
12. Lutsenko S, Bhattacharjee A, Hubbard AL. Copper handling machinery of the brain. *Metallomics.* 2010;2:596–608.
13. Jones PW, Taylor DM, Williams DR. Analysis and chemical speciation of copper and zinc in wound fluid. *J Inorg Biochem.* 2000;81:1–10.
14. Mirastschijski U, Martin A, Jorgensen LN, Sampson B, Agren MS. Zinc, copper, and selenium tissue levels and their relation to subcutaneous abscess, minor surgery, and wound healing in humans. *Biol Trace Elem Res.* 2013;153:76–83.
15. Sen CK, Khanna S, Venojarvi M, et al. Copper-induced vascular endothelial growth factor expression and wound healing. *Am J Physiol Heart Circ Physiol.* 2002;282:H1821–H1827.
16. Zheng Z, White C, Lee J, et al. Altered microglial copper homeostasis in a mouse model of Alzheimer's disease. *J Neurochem.* 2010;114:1630–1638.
17. Noshita N, Sugawara T, Hayashi T, et al. Copper/zinc superoxide dismutase attenuates neuronal cell death by preventing extracellular signal-regulated kinase activation after transient focal cerebral ischemia in mice. *J Neurosci.* 2002;22:7923–7930.
18. Lewén A, Sugawara T, Gasche Y, Fujimura M, Chan PH. Oxidative cellular damage and the reduction of APE/Ref-1 expression after experimental traumatic brain injury. *Neurobiol Dis.* 2001;8:380–390.
19. Cole JT, Angela Y, Kean WS, et al. Craniotomy: true sham for traumatic brain injury, or a sham of a sham? *J Neurotrauma.* 2011;28:359–369.
20. Homsi S, Piaggio T, Croci N, et al. Blockade of acute microglial activation by minocycline promotes neuroprotection and reduces locomotor hyperactivity after closed head injury in mice: a twelve-week follow-up study. *J Neurotrauma.* 2010;27:911–921.
21. Lighthall JW. Controlled cortical impact: a new experimental brain injury model. *J Neurotrauma.* 1988;5:1–15.
22. Kernie SG, Erwin TM, Parada LG. Brain remodeling due to neuronal and astrocytic proliferation following controlled cortical injury in mice. *J Neurosci Res.* 2001;66:317–326.
23. Gatson JW, Liu MM, Abdelfattah K, et al. Estrone is neuroprotective in rats after traumatic brain injury. *J Neurotrauma.* 2012;29:2209–2210.
24. Cowell RM, Plane JM, Silverstein FS. Complement activation contributes to hypoxic–ischemic brain injury in neonatal rats. *J Neurosci.* 2003;23:9459–9468.
25. Peng F, Lutsenko S, Sun X, Muzik O. Positron emission tomography of copper metabolism in the $Atp7b^{-/-}$ knock-out mouse model of Wilson's disease. *Mol Imaging Biol.* 2012;14:70–78.
26. Cai H, Wu J, Muzik O, Hsieh J, Lee R, Peng F. Reduced ^{64}Cu uptake and tumor growth inhibition by knockdown of human copper transporter 1 in xenograft mouse model of prostate cancer. *J Nucl Med.* 2014;55:622–628.
27. Chuang N, Mori S, Yamamoto A, et al. An MRI-based atlas and database of the developing mouse brain. *Neuroimage.* 2011;54:80–89.
28. Loening AM, Gambhir SS. AMIDE: a free software tool for multimodality medical image analysis. *Mol Imaging.* 2003;2:131–137.
29. Ito D, Imai Y, Ohsawa K, et al. Microglia-specific localization of a novel calcium binding protein, Iba1. *Mol Brain Res.* 1998;57:1–9.
30. Zhang H, Cai H, Lu X, Muzik O, Peng F. Positron emission tomography of human hepatocellular carcinoma xenografts in mice using copper (II)-64 chloride as a tracer with copper (II)-64 chloride. *Acad Radiol.* 2011;18:1561–1568.
31. Converse AK, Larsen EC, Engle JW, et al. ^{11}C-(R)-PK11195 PET imaging of microglial activation and response to minocycline in zymosan-treated rats. *J Nucl Med.* 2011;52:257–262.
32. Wang Y, Yue X, Kiesewetter DO, Niu G, Teng G, Chen X. PET imaging of neuroinflammation in a rat traumatic brain injury model with radiolabeled TSPO ligand DPA-714. *Eur J Nucl Mol Imaging.* 2014;41:1440–1449.
33. Wang LM, Becker JS, Wu Q, et al. Bioimaging of copper alterations in the aging mouse brain by autoradiography, laser ablation inductively coupled plasma mass spectrometry and immunohistochemistry. *Metallomics.* 2010;2:348–353.
34. Matusch A, Depboylu C, Palm C, et al. Cerebral bioimaging of Cu, Fe, Zn, and Mn in the MPTP mouse model of Parkinson's disease using laser ablation inductively coupled plasma mass spectrometry. *J Am Soc Mass Spectrom.* 2010;21:161–171.
35. Bush JA, Mahoney JP, Markowitz H, Gubler CJ, Cartwright GE, Wintrobe MM. Studies on copper metabolism. XVI. Radioactive copper studies in normal subjects and in patients with hepatolenticular degeneration. *J Clin Invest.* 1955;34: 1766–1778.
36. Osborn SB, Szaz KF, Walshe JM. Studies with radioactive copper (^{64}Cu and ^{67}Cu): abdominal scintiscans in patients with Wilson's disease. *Q J Med.* 1969;38:467–474.
37. Walshe JM, Potter G. The pattern of the whole body distribution of radioactive copper (^{67}Cu, ^{64}Cu) in Wilson's disease and various control groups. *Q J Med.* 1977;46:445–462.
38. Trumbo P, Yates AA, Schlicker S, Poos M. Dietary reference intakes: vitamin A, vitamin K, arsenic, boron, chromium, copper, iodine, iron, manganese, molybdenum, nickel, silicon, vanadium, and zinc. *J Am Diet Assoc.* 2001;101:294–301.
39. Choi BS, Zheng W. Copper transport to the brain by the blood-brain barrier and blood-CSF barrier. *Brain Res.* 2009;1248:14–21.